RSC Advances

PAPER

View Article Online
View Journal | View Issue

Cite this: *RSC Adv.*, 2020, **10**, 19974

Anthracene derivatives as broadband nonlinear optical materials: nonlinear absorption and excited-state dynamics analysis†

Wenfa Zhou,[a] Yu Fang,[b] Xingzhi Wu,[b] Yanbing Han,[c] Junyi Yang,*[d] Lei Shen[d] and Yinglin Song*[cd]

Two anthracene derivatives, **AN-1** and **AN-2**, with different π-bridge lengths were designed and synthesized to investigate their optical nonlinearities. The nonlinear absorption (NLA) properties of both derivatives were measured *via* the femtosecond Z-scan technique with the wavelength range from 532 nm to 800 nm. The reverse saturable absorption (RSA) of both compounds results from two-photon absorption induced excited-state absorption (TPA-ESA). At all wavelengths, the reverse saturable absorption of **AN-2** is superior to that of **AN-1** due to a better molecular planarity for **AN-2**. Compared with the results of **AN-1**, the two-photon absorption coefficient of **AN-2** can be increased by nearly 8 times (from 0.182 × 10^{-2} cm GW^{-1} for **AN-1** to 1.42 × 10^{-2} cm GW^{-1} for **AN-2**) at 600 nm by extending the π-bridge. The evolution of femtosecond transient absorption (TA) spectra reveals the relaxation process from the singlet local excited-state (LES) to charge transfer state (CTS) for both compounds. The results imply that anthracene derivatives may be potential candidates for applications in future laser photonics.

Received 22nd March 2020
Accepted 18th May 2020

DOI: 10.1039/d0ra02638g

rsc.li/rsc-advances

1 Introduction

In recent decades, organic materials have attracted increasing attention in the fields of optoelectronics and photonics. They have been used in various practical applications, such as optical limiters, all-optical switches, organic light-emitting diodes, *etc.*[1–8] Previous studies have revealed that the nonlinear optical (NLO) response is dependent on the strength of the donor and acceptor, the extension of the π-conjugated length and the planarity of the π-conjugated system.[9–13] Although a variety of organic materials have been synthesized, and the NLO characteristics have been presented, there are still many unknown relationships between these structures and their properties. It is vital to investigate the NLO properties of new π-conjugated molecules to optimize their structures and enhance their NLO response.

Among the wide variety of π-centers used, we considered anthracene to be a potential conjugated π-center not only because it is planar but also because it is convenient to effectively adjust its electronic and photonic properties due to the nature of the active groups and how they are linked.[14–16] Previous studies have indicated that anthracene derivatives exhibit excellent NLO response,[17,18] but few studies have been conducted on their internal photophysical mechanisms. On the one hand, some researchers have reported that intramolecular charge transfer (ICT) is significant for obtaining two-photon absorption (TPA) chromophores with large TPA cross sections, and these molecules may be potential candidates for using as two-photon materials and optical limiters in laser photonics.[19–22] On the other hand, Planells *et al.* reported that a small torsion angle improved the planarity of the molecule and enhanced the NLO response.[23] Therefore, not only the strength of the donor or acceptor but also the planarity of the molecule can influence the NLO response. Our previous work revealed that extending the π-conjugated length and molecules with a better π-conjugated planar shows obvious enhancement of the NLO response.[24,25]

From the perspective of molecular planarity, two anthracene derivatives with different π-bridge were synthesized (Fig. 1): (*E*)-3-(anthracen-9-yl)-1-(4-(dimethylamino)phenyl)prop-2-en-1-one (**AN-1**) and (2*E*,4*E*)-5-(anthracen-9-yl)-1-(4-(dimethylamino) phenyl)penta-2,4-dien-1-one (**AN-2**). Compared to the structure of **AN-1**, the structure of **AN-2** contained one more ethylene double bonds, which extended the length of the π-bridge. Using the femtosecond Z-scan technique, the NLO responses of these derivatives were studied, and the mechanism was analysed. The magnitude and sign of nonlinear absorption coefficients for **AN-**

[a]*School of Optoelectronic Science and Engineering, Soochow University, Suzhou 215006, China*

[b]*Jiangsu Key Laboratory of Micro and Nano Heat Fluid Flow Technology and Energy Application, School of Mathematics and Physics, Suzhou University of Science and Technology, Suzhou 215009, China*

[c]*Department of Physics, Harbin Institute of Technology, Harbin 150001, China. E-mail: ylsong@hit.edu.cn*

[d]*School of Physical Science and Technology, Soochow University, Suzhou 215006, China. E-mail: yjy2010@suda.edu.cn*

† Electronic supplementary information (ESI) available. See DOI: 10.1039/d0ra02638g

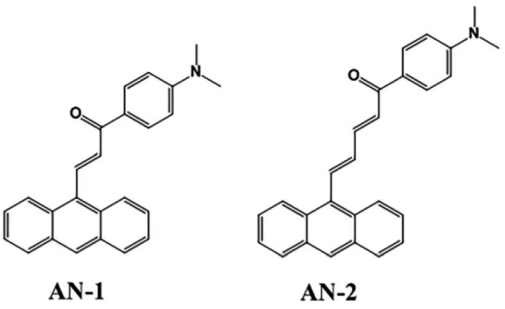

Fig. 1 Chemical structures of (*E*)-3-(anthracen-9-yl)-1-(4-(dimethylamino)phenyl)prop-2-en-1-one (**AN-1**) and (2*E*,4*E*)-5-(anthracen-9-yl)-1-(4-(dimethylamino)phenyl)penta-2,4-dien-1-one (**AN-2**).

1 and **AN-2** were obtained. The evolution of the TA spectra indicated that the relaxation process of the particles in **AN-1** and **AN-2** was the transition from the local excited-state (LES) to the charge transfer state (CTS). Our results show that extending the π-bridge *via* increasing the amount of ethylene can adjust the molecular planarity, which can enhance the nonlinear absorption (NLA) response.

2 Experiments and theoretical calculation

2.1 Synthesis of AN-1 and AN-2

Synthesis of (*E*)-3-(anthracen-9-yl)-1-(4-(dimethylamino) phenyl)prop-2-en-1-one (AN-1). The mixture of 9-anthraldehyde (206 mg, 1 mmol) and 4′-dimethylaminoacetophenone (163 mg, 1 mmol) were dissolved in 20 mL of ethanol. The PH was adjusted to 7–8 with 1 sodium hydroxide (NaOH, 10%) solution. The reaction system was stirred for 10 h at room temperature. After washing the crude product three times with ethanol, the residue was separated through a column chromatography (silica gel) with petroleum ether/dichloromethane (v/v, 8 : 1). The yield was 78%. ^{1}H NMR δ/ppm (400 MHz, DMSO) δ 8.66 (s, 1H), 8.53 (d, J = 15.8 Hz, 1H), 8.23 (t, J = 14.1 Hz, 1H), 8.15 (d, J = 8.6 Hz, 1H), 8.03 (d, J = 8.8 Hz, 1H), 7.68 (t, J = 16.7 Hz, 1H), 7.58 (p, J = 6.8 Hz, 2H), 6.77 (d, J = 8.8 Hz, 1H), 3.04 (s, 3H). See ESI Fig. S1† (Fig. 2).

Synthesis of (2*E*,4*E*)-5-(anthracen-9-yl)-1-(4-(dimethylamino) phenyl)penta-2,4-dien-1-one (AN-2). The mixture of 3-(9-anthryl)acrolein (232 mg, 1 mmol) and 4′-dimethylaminoacetophenone (163 mg, 1 mmol) were dissolved in 20 mL of ethanol. The PH was adjusted to 7–8 with sodium hydroxide (NaOH, 10%) solution. The reaction system was stirred for 16 h at room temperature. After washing the crude product three times with ethanol, the residue was separated through a column chromatography (silica gel) with petroleum ether/dichloromethane (v/v, 8 : 1). The yield was 72%. ^{1}H NMR δ/ppm (400 MHz, DMSO) δ 8.61 (s, 1H), 8.34 (d, J = 7.0 Hz, 1H), 8.12 (s, 1H), 7.97 (d, J = 7.9 Hz, 1H), 7.79 (t, J = 12.5 Hz, 1H), 7.57 (s, 1H), 7.15–6.93 (m, 1H), 6.77 (d, J = 7.2 Hz, 1H), 3.04 (s, 1H). See ESI Fig. S2.†

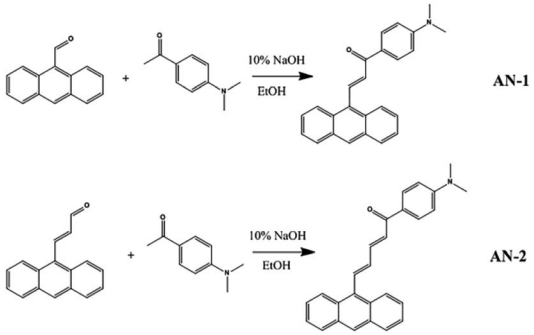

Fig. 2 Synthetic scheme of **AN-1** and **AN-2**.

2.2 Z-scan experiment

The nonlinear absorption of **AN-1** and **AN-2** was measured by the open-aperture Z-scan method.[26] The light source was an optical parametric amplifier (OPA, Light Conversion ORPHEUS, 190 fs, 20 Hz) pumped by a mode-locked Yb:KGW-based fiber laser. The output wavelength of OPA was tuned from 532 nm to 800 nm. The spatial and temporal distributions of the pulse were all nearly Gaussian profiles. A dimethyl sulfoxide (DMSO) solution at a concentration of 4.3×10^{-3} mol L^{-1} contained in 2 mm quartz cells was used as the sample. The beam waist radii were 24.5 μm at 532 nm, 25.4 μm at 560 nm, 27.1 μm at 600 nm, 31.6 μm at 700 nm and 35.7 μm at 800 nm, respectively.

2.3 Transient absorption measurement

The wavelength of 400 nm fs pulse output from the OPA was used as pump pulse. The probing beams of the white light supercontinuum from sapphire crystal covered from 465 nm to 765 nm. In the experiment, the laser pulse width was 190 fs with the repetition rate of laser pulse was 6 kHz. The time resolution of the experimental system used is approximately 250 fs. The solutions in 2 mm quartz cells were used as samples.

2.4 Quantum chemical calculations

The Gaussian 09 program package was used for density functional theory (DFT). The B3LYP/6-31G model was employed to optimize the structures of all the molecular systems.[27] The energy and electron cloud distribution of frontier molecular orbitals were calculated (Fig. 3). The possession percentage of each component at frontier molecular orbitals was determined by Gauss Sum[28] (Table 1).

In both compounds, the electrons transfer from donor (anthracene group) to acceptor (dimethylaminoacetophenone group). The possession percentage changing from the highest occupied molecular orbital (HOMO) to the lowest unoccupied molecular orbital (LUMO) of the anthracene group in **AN-1** changed from 91% to 75%, while that in **AN-2** changed from 82% to 59%. The results show that there were obvious π–π* transition features in both molecules. Moreover, the possession percentage (changes from HOMO to LUMO) of the acceptor for **AN-1** changes from 7% to 19%, while that for **AN-2** changes from 8% to 21%. Both molecules exhibited ICT. Compared with the structure of **AN-1**, the π-bridge length in **AN-2** was extended, which may lead to the molecular conformation to change due to

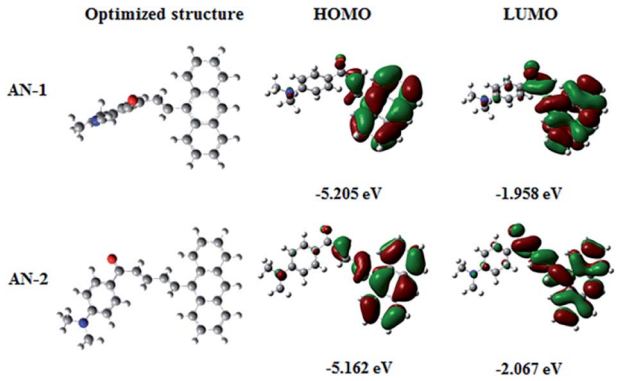

Fig. 3 The optimized structure and frontier molecular orbital distributions of AN-1 and AN-2 extracted from DFT calculation.

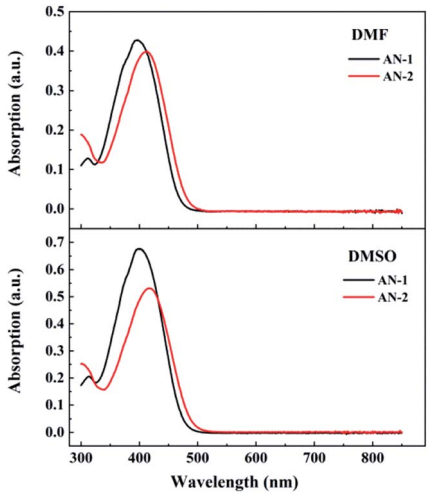

Fig. 4 UV-vis absorption spectra of AN-1(black lines) and AN-2 (red lines) dissolved in DMSO and DMF solutions.

the steric effects. As shown in the DFT optimized structure in Fig. 3, the torsion angles between donor and acceptor for **AN-1** and **AN-2** were approximately 103° and 22°, respectively. It indicated that the molecular planarity of **AN-2** is better than that of **AN-1**, which is consistent with our original molecular design idea. Generally, molecules with better plane exhibit large optical nonlinear responses.[20,23,25,29,30]

3 Results and discussion

3.1 UV-vis absorption spectra

The UV-vis absorption spectra of compounds **AN-1** and **AN-2** were investigated in the solvents of different polarities at room temperature (Fig. 4). The concentration of compounds **AN-1** and **AN-2** dissolved in dimethyformamide (DMF) and DMSO were on the order of 10^{-5} mol L^{-1}, respectively. The similar absorption broad absorption profiles with low-energy maxima suggested the existence of ICT. **AN-1** and **AN-2** dissolved in DMSO display maximum absorption peaks at 400 nm and 420 nm, respectively. With excitation at the maximum absorption wavelength, no fluorescence signal was observed for both materials, which caused by charge transfer and implied that ultrafast non-radiative deactivation is the mainly decay way of the excited state. As shown in Fig. 3, the HOMO–LUMO gap of both anthracene derivatives can be obtained (3.247 eV for **AN-1** and 3.095 eV for **AN-2**). Then, the position of the maximum absorption peaks can be calculated and it was consistent with the results of UV-vis absorption. Compared to the absorption peak of **AN-1**, the absorption peak of **AN-2** is approximately 20 nm red shifted, which could be attributed to the decrease in the energy HOMO–LUMO gap, and implies that the effective π-conjugated length of **AN-2** may be larger than that of **AN-1**.[31]

3.2 Open aperture Z-scan experiment

A femtosecond Z-scan was carried out to study the NLO properties of both anthracene derivatives. The excitation wavelengths were covered a broadband range from 532 nm to 800 nm, which belonged to the off-resonance range. Both compounds displayed high linear transmittance (**AN-1** ≥ 97% and **AN-2** ≥ 90%). Here, three wavelengths (532 nm, 600 nm, 800 nm) were selected as examples to show the difference of strength of NLA between **AN-1** and **AN-2** (Fig. 5). The experimental data are fitted by Sheik Bahae's theory.[26] All these results are summarized in Table 2. The observed NLA of both compounds was evaluated to originate from the solution molecule because the pure solvent displayed no NLA in the experimental conditions. Obviously, both compounds exhibit reverse saturable absorption (RSA), and the reverse saturable absorption (RSA) of **AN-2** is stronger than that of **AN-1** at all excited wavelengths. The effective nonlinear absorption coefficients of **AN-2** are approximately 3–5 times greater than that of **AN-1** with the same intensity at each wavelength.

Table 1 The possession percentage of each component occupied in frontier molecular orbitals of AN-1 and AN-2

	AN-1 (%)			**AN-2** (%)		
	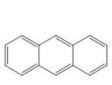		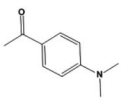	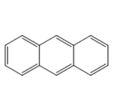	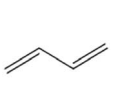	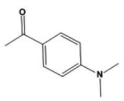
LUMO	75	6	19	59	20	21
HOMO	91	2	7	82	10	8

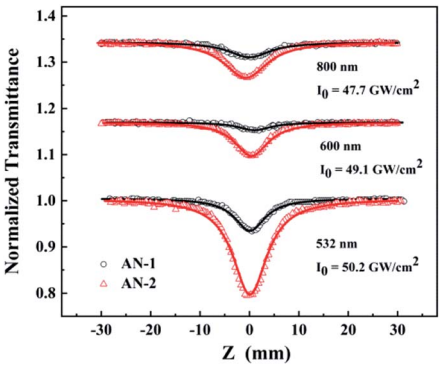

Fig. 5 Open-aperture Z-scan experiment under 190 fs at 532 nm, 600 nm, and 800 nm. Circles and triangles are experimental data. Solid lines represent the theoretical fitting.

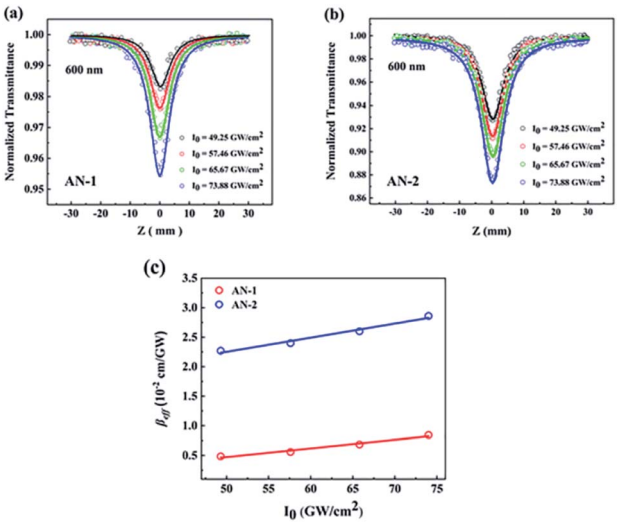

Fig. 6 The results of the open-aperture Z-scan at 600 nm for (a) **AN-1** and (b) **AN-2**. The solid lines represent theoretical fitting. (c) Nonlinear absorption coefficients as a function of input intensity at 600 nm for **AN-1** and **AN-2**.

Since high linear transmittance was measured at all excitation wavelengths and the femtosecond laser pulse was used as light source, we consider that TPA could be the main mechanism. To further analyze the optical nonlinear mechanisms for both compounds, open-aperture Z-scan measurements at different intensities I_0 for both compound solutions at all excited wavelengths were performed (Fig. S3 and S4†). Through numerical fitting, it can be found that the effective nonlinear absorption coefficients β_{eff} grow linearly with incident intensity under photoexcitation for each wavelength. Here, take the experimental results at 600 nm as an example. By theoretical fitting, the effective nonlinear absorption coefficients β_{eff} at different intensities I_0 were obtained (Fig. 6). These results indicate that TPA is not the only mechanism because TPA coefficients are independent of the intensity.[32,33] We considered that there was higher-order NLA. In order to further analyze the mechanism of NLA in both materials, femtosecond TA was conducted by using a 190 fs pump pulse with a wavelength of 400 nm. The results show that the positive signal appeared in a range from 465 nm to 765 nm (Fig. 7), which resulted from ESA. We considered that the higher-order NLA can be assigned as TPA-induced ESA (TPA-ESA).[25,30]

In general, organic molecules may display both TPA and TPA-ESA processes under off-resonant excitation.[34,35] Generally, the expression of the absorption coefficient of materials with TPA-ESA can be expressed as $\alpha = \alpha_0 + \beta I + \gamma I^2$. Herein, α_0 represents the linear absorption coefficient. β and γ represent TPA and the effective fifth-order nonlinear absorption coefficient, respectively. The TPA cross section σ_{TPA} can be obtained with the expression of $\sigma_{TPA} = \hbar\omega\beta/N$.[30] Here, $\hbar$ and ω are reduced Planck constant and angular frequency, respectively. β is the TPA coefficient, and N is the population density in unit volume. All the results are summarized in Table 3. For **AN-2**, a better molecular planarity in **AN-2** not only increased the effective π-conjugation length of molecule but also enhanced the charge delocalization extent, which could be conducive to charge transfer. This could be main reason that the TPA coefficients of **AN-2** are larger than that of **AN-1**.[36,37] Here, the TPA coefficients of both compounds at 800 nm were larger than that at 600 nm, which may be attributed to two-photon resonance of at $S_0 \rightarrow S_1$ transition.

In addition, comparing the TPA coefficients of both compounds at 532 nm with other organic materials, it is superior to the previously reported nonlinear materials (Table 4). It reveals that extending the π-bridge to adjust the molecular planarity *via* increasing the amount of ethylene can greatly modulate the strength of NLA.

3.3 Transient absorption spectra

To further investigate the mechanism of the photophysical process for both compounds under photoexcitation in detail, TA spectra of two materials were obtained at a pump pulse wavelength of 400 nm (Fig. 7). The changes in the absorption intensity at specific wavelengths obtained from transient

Table 2 Parameters of femtosecond open-aperture Z-scan experiments at 532 nm, 600 nm and 800 nm

Wavelength (nm)	I_0 (GW cm^{-2})	**AN-1** $\beta_{eff} \times 10^{-2}$ (cm GW^{-1})	**AN-2** $\beta_{eff} \times 10^{-2}$ (cm GW^{-1})
532	50.2	2.15	8.35
600	49.1	0.48	2.3
800	47.7	1.07	2.38

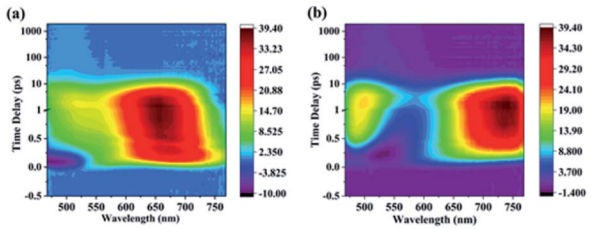

Fig. 7 TA spectra of (a) **AN-1** and (b) **AN-2** excited at the wavelength of 400 nm.

absorption spectra experiments are represented by changes in optical density (ΔOD), which can be expressed as follows:

$$\Delta OD = -\lg(T/T_0) \quad (1)$$

Here, T is the transmittance of the sample after pumping, and T_0 is the linear transmittance of the sample. The positive signal represents RSA, while the negative signal represents saturable absorption. Several absorptive spectra are selected at different delay times to discuss the changed process of the spectra for **AN-1** and **AN-2** (Fig. 8). The results show that a positive signal appeared in the wavelength range from 465 nm to 765 nm for both compounds, which can be regarded as ESA. Moreover, broadband RSAs are observed in both compounds. For **AN-1**, two signal bands appear near zero delay time, namely, a negative signal band centered at 475 nm and a positive signal band peaking at 575 nm and 710 nm. As the time delay became longer, the negative signal band gradually disappeared, and the absorption peak of the positive signal band exhibited a blue shift. The absorption peak of the positive signal band stabilized at 500 nm and 650 nm, after which the amplitude of spectra for **AN-1** attenuated according to this waveform. However, after dozens of picoseconds, the profile of the spectra varied, leaving only an absorption peak with a central wavelength of 500 nm. The generation and disappearance of the negative signal is caused by the combination of ground state bleaching and excited-state absorption. The spectral change of **AN-2** is similar to that of **AN-1**. First, the absorption peak of its positive signal band stabilized at 500 nm and 740 nm, after which the amplitude of its spectra attenuated according to this waveform. This spectral form changed after dozens of picoseconds, leaving only an absorption peak with a center wavelength of 525 nm. The spectral changes of **AN-1** and **AN-2** mean that ESA does not originated from the same excited-state.[40,41] Compared to the transient absorption peak of **AN-1**, the transient absorption peak of **AN-2** exhibited a redshift, which indicated the impact of the extended π-bridge on the ESA of anthracene compounds.

The dynamics of **AN-1**(480 nm, 500 nm and 532 nm) and **AN-2** (500 nm, 532 nm and 550 nm) after photoexcitation were extracted from the transient absorption spectra to analyze the relaxation process, as shown in Fig. 9. The transient photodynamic traces for **AN-1** and **AN-2** can be depicted by a convolution of three e-exponential functions and instrument response curves following this fitting equation:

$$\Delta T(t) = \sum_{i=1,n}\int_{-\infty}^{\infty} R_{IRF}(\tau)\left[A_i \exp\left(-\frac{t-\tau}{\tau_i}\right)\right]d\tau = R_{IRF} \otimes \left[\sum_{i=1,n} A_i \exp\left(-\frac{t}{\tau_i}\right)\right] \quad (2)$$

where $\Delta T(t)$ and R_{IRF} are the normalized transient absorption signal and instrument response curve, respectively. τ_i and A_i represent the time and amplitude terms of the e-exponential function, respectively. ⊗ is the convolution operation. The parameters for the two anthracene derivatives are summarized in Table 5. According to the results of quantum chemical calculations, both compounds exhibited ICT, which could activate the NLO response. Therefore, the NLO responses were the result of the relaxation of particles from the singlet local excited-state (LES) to the charge transfer state (CTS). Due to the resonance excitation (400 nm), the mechanism of positive nonlinear absorption is excited-state absorption induced by one-photon absorption. We tend to consider the singlet ESA and choose a simplified energy model to demonstrate the excited-state dynamics (Fig. 10).

Under photoexcitation, particles transition to LES, and there may be three relaxation processes: (1) since the waveform of spectra for both compounds did not change within several picoseconds, the particles were in the same excited-state and we considered that the first relaxation process could be regarded as the establishment of LES and the vibrational cooling relaxation in the LES with a lifetime of τ_1. (2) The amplitude of the spectrum attenuated after a several picoseconds until there was only one absorption peak remaining, which indicated that the particles relaxed from the LES to the CTS with the time of τ_2. The charge transfer may lead to fluorescence quenching.[42–44] (3) The long lifetime (τ_3) was the time that particles slowly decayed back from CTS to ground state S_0. Our results show that **AN-1**

Table 3 Parameters of NLA at different wavelengths extracted from femtosecond open-aperture Z-scan

	AN-1			**AN-2**		
Wavelength (nm)	β $\times 10^{-2}$ (cm GW^{-1})	σ_{TPA} (GM)	γ $\times 10^{-4}$ (cm^3 GW^{-2})	β $\times 10^{-2}$ (cm GW^{-1})	σ_{TPA} (GM)	γ $\times 10^{-4}$ (cm^3 GW^{-2})
532	1.28	184.9	3	5.63	813.1	15
560	0.712	97.7	2	3.42	469.3	10
600	0.182	23.3	1.5	1.42	181.9	3.5
700	0.336	36.9	2.13	0.667	73.2	6.5
800	0.625	60	1.6	1.54	147.9	4.3

Table 4 Comparison of the TPA coefficients for **AN-1** and **AN-2** at 532 nm with literature data

	$\beta \times 10^{-2}$ (cm GW^{-1})	Wavelength (nm)	Concentration (mol L^{-1})	Laser pulse (fs)
AN-1	1.28	532	0.0043	190
AN-2	5.63	532	0.0043	190
DBPy[25]	0.7	532	0.002	190
P2 (ref. 30)	1.0	532	0.0137	190
15#[38]	1.6	500	0.01	200
L1 (ref. 39)	2.5	532	0.01	190

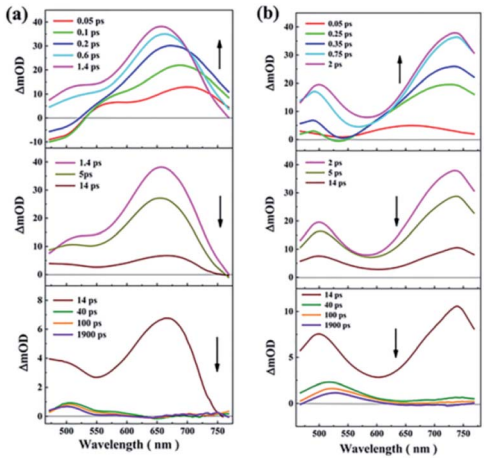

Fig. 8 Several TA spectra of (a) **AN-1** and (b) **AN-2** at selected delay times are displayed.

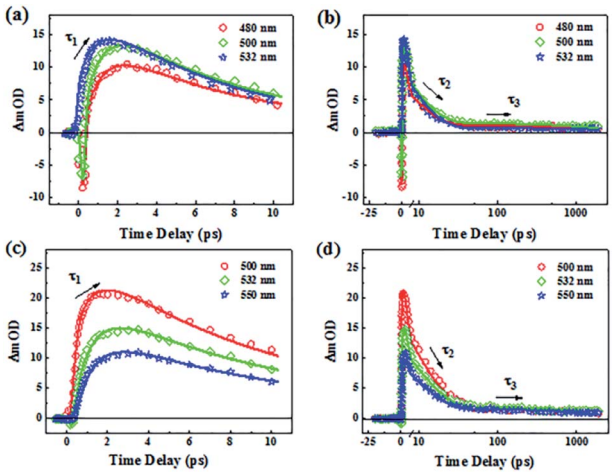

Fig. 9 The dynamic traces of **AN-1** at a short delay time (a) and a long delay time (b). The dynamic traces of **AN-2** at a short delay time (c) and a long delay time (d). Solid lines are theoretical fitting. The solid lines are theoretical fitting.

and **AN-2** has different excited-state lifetimes, and it revealed that increasing the amount of ethylene double bonds to extend the π-bridge in these compounds can also modulate the TA spectra.

Table 5 Fitting results of dynamics traces for **AN-1** and **AN-2** after photoexcitation

	τ_1 (ps)	τ_2 (ps)	τ_3 (ns)
AN-1	0.89	7.02	1.84
AN-2	0.92	8.86	2.27

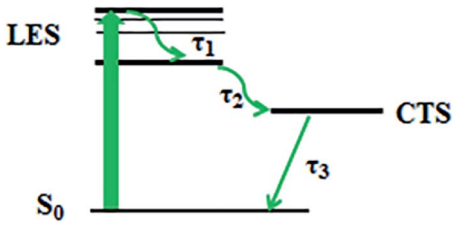

Fig. 10 The energy relaxation diagram for **AN-1** and **AN-2**.

4 Conclusions

The NLO properties of two novel anthracene derivatives were studied in the off-resonant region. The multi-wavelength femtosecond Z-scan results show that both derivatives exhibit good RSA responses, and the RSA of **AN-2** is stronger than that of **AN-1**, which is related to the better molecular planarity. By theoretical fitting, the difference of the TPA coefficients between **AN-1** and **AN-2** was nearly 8 times (from 0.182 × 10^{-2} cm GW^{-1} for **AN-1** to 1.42 × 10^{-2} cm GW^{-1} for **AN-2**) at 600 nm. Furthermore, the TPA coefficients of both compounds at 532 nm were compared with reported organic materials. Further dynamics analysis was performed, and the photophysical parameters of both compounds were obtained. The difference of the NLA response between **AN-1** and **AN-2** implied that extending the π-bridge to adjust the molecular planarity *via* increasing the amount of ethylene can modulate the NLO response. The experimental results imply that anthracene derivatives are potential NLO materials that can be used in future optoelectronics.

Conflicts of interest

There are no conflicts to declare.

Acknowledgements

This study was funded by the NSAF (Grant No. U1630103), Special Fund from State Key Laboratory of Intense Pulsed Radiation Simulation and Effect (No. SKLIPR1715), National Natural Science Foundation of China (No. 11704273, 11804244), Natural Science Foundation of Jiangsu Province, China (Grant No. BK20180965, BK20170375), Natural Science Foundation of the Jiangsu Higher Education Institutions of China (Grant No. 17KJB140021).

References

1 T. Qin, W. Wiedemair, S. Nau, R. Trattnig, S. Sax, S. Winkler, A. Vollmer, N. Koch, M. Baumgarten, E. List and K. Müllen. Core, Shell, and Surface-Optimized Dendrimers for Blue Light-Emitting Diodes, *J. Am. Chem. Soc.*, 2011, **133**(5), 1301–1303.

2 S. Lai, Q. Tong, M. Chan, T. Ng, M. Lo, S. Lee and C. Lee, Distinct electroluminescent properties of triphenylamine derivatives in blue organic light-emitting devices, *J. Mater. Chem.*, 2011, **21**(4), 1206–1211.

3 Y. Liu, C. Li, Z. Ren, S. Yan and M. Bryce, All-organic thermally activated delayed fluorescence materials for organic light-emitting diodes, *Nat. Rev. Mater.*, 2018, **3**, 18020.

4 D. Li, Y. Hu and L. Liao, Triplet exciton harvesting by multi-process energy transfer in fluorescent organic light-emitting diodes, *J. Mater. Chem. C*, 2019, **7**, 977–985.

5 B. Gao, L. Mazur, M. Morshedi, A. Barlow, H. Wang, C. Quintana, C. Zhang, M. Samoc, M. Cifuentes and M. Humphrey, Exceptionally large two- and three-photon absorption cross-sections by OPV organometalation, *Chem. Commun.*, 2016, **52**, 8301–8304.

6 K. Manjunatha, R. Rajarao, G. Umesh, B. Bhat and P. Poornesh, Optical nonlinearity, limiting and switching characteristics of novel ruthenium metal-organic complex, *Opt. Mater.*, 2017, **72**, 513–517.

7 A. Almosawe and H. Saadon, Nonlinear optical and optical limiting properties of new structures of organic nonlinear optical materials for photonicapplications, *Chin. Opt. Lett.*, 2013, **11**(4), 041902.

8 P. Patil, S. Maidur, S. Venugopal and S. Dharmaprakash, Crystalline perfection, third-order nonlinear optical properties and optical limiting studies of 3,4-dimethoxy-4′-methoxychalcone single crystal, *Opt. Laser Technol.*, 2016, **81**, 70–76.

9 K. Kim, S. Noh, T. Katsuda, S. Ito, A. Osuka and D. Kim, Charge transfer induced enhancement of near-IR two-photon absorption of 5,15-bis(azulenylethynyl) zinc(ii) porphyrins, *Chem. Commun.*, 2007, **24**, 2479–2481.

10 S. Shettigar, P. Poornesh, G. Umesh, B. Sarojini, B. Narayana and K. Kamath, Investigation of third-order nonlinear optical properties of conjugated benzodioxal derivatives, *Opt. Laser Technol.*, 2010, **42**(7), 1162–1166.

11 X. Zhan, J. Zhang, S. Tang, Y. Lin, M. Zhao, J. Yang, H. Zhang, Q. Peng, G. Yu and Z. Li, Pyrene fused perylene diimides: synthesis, characterization and applications in organic filed-effect transistors and optical limiting with high performance, *Chem. Commun.*, 2015, **51**, 7156–7159.

12 B. Coe, D. Rusanova, V. Joshi, S. Sánchez, J. Vávra, D. Khobragade, L. Severa, I. Cĺsařová, D. Šaman, R. Pohl, K. Clays, G. Depotter, B. Brunschwig and F. Teplý, Helquat dyes: helicene-like push–pull systems with large second-order nonlinear optical responses, *J. Org. Chem.*, 2016, **81**(5), 1912–1920.

13 Z. Jin, D. Wang, X. Wang, P. Liang, Y. Mi and H. Yang, Efficient modification of pyrene-derivative featuring third-order nonlinear optics via the click post-functionalization, *Tetrahedron Lett.*, 2013, **54**(36), 4859–4864.

14 W. Yang, M. Seo, X. Wang, S. Jeon and B. Cho, Two-photon Absorption Properties of 9,10-Disubstituted 2,6-Bis(p-dihexylaminostyryl)anthracene Derivatives. Effect of 9,10-Substituents, *J. Fluoresc.*, 2008, **18**(2), 403–411.

15 W. Yang, D. Kim, M. Jeong, H. Kim, S. Jeon and B. Cho, 2,6-Bis(styryl)anthracene Derivatives with Large Two-Photon Cross-Sections, *Chem. Commun.*, 2003, **20**, 2618–2619.

16 L. Bu, Y. Li, J. Wang, M. Sun, M. Zheng, W. Liu, S. Xue and W. Yang, Synthesis and piezochromic luminescence of aggregation-enhanced emission 9,10-bis(N-alkylcarbazol-2-yl-vinyl-2)anthracenes, *Dyes Pigm.*, 2013, **99**(3), 833–838.

17 L. Li, Y. Wu and Y. Wang, Nonlinear two-photon absorption properties induced by femtosecond laser with the films of two novel anthracene derivatives, *Chin. Opt. Lett.*, 2012, **10**, 101602.

18 S. Maidur, J. Jahagirdar, P. Patil, T. Chia and C. Quah, Structural characterizations, Hirshfeld surface analyses, and third-order nonlinear optical properties of two novel chalcone derivatives, *Opt. Mater.*, 2018, **75**, 580–594.

19 W. Yang, D. Kim, M. Jeong, H. Kim, Y. Lee, X. Fang, S. Jeon and B. Cho, Two-Photon Absorption Properties of 2,6-Bis(styryl)anthracene Derivatives: Effects of Donor–Acceptor Substituents and the π Center, *Chemistry*, 2005, **11**(14), 4191–4198.

20 H. Zhang, E. Guo, Y. Zhang, P. Ren and W. Yang, Donor–Acceptor-Substituted Anthracene-Centered Cruciforms: Synthesis, Enhanced Two-Photon Absorptions, and Spatially Separated Frontier Molecular Orbitals, *Chem. Mater.*, 2009, **21**(21), 5125–5135.

21 P. Patil, S. Maidur, J. Jahagirdar, T. Chia, C. Quah and M. Shkir, Crystal structure, spectroscopic analyses, linear and third-order nonlinear optical properties of anthracene-based chalcone derivative for visible laser protection, *Appl. Phys. B*, 2019, **125**, 163.

22 Y. Zhang, P. Ren, H. Zhan, E. Guo and W. Yang, 9,10-Anthracene-centered oligo(p-phenyleneethynylene)s with end-capping didecylamines exhibiting enhanced two-photon fluorescence action cross-section, *J. Lumin.*, 2010, **130**(3), 527–530.

23 M. Planells, M. Pizzotti, G. Nichol, F. Tessore and N. Robertson, Effect of torsional twist on 2nd order non-linear optical activity of anthracene and pyrene tricyanofuran derivatives, *Phys. Chem. Chem. Phys.*, 2014, **16**, 23404–23411.

24 Q. Xu, Z. Li, N. Liu, J. Jia, J. Yang and Y. Song, Third order nonlinear optical properties and transient dynamics of thiophene-contained pyrene derivatives: effect of peripheral substituent group, *Opt. Laser Technol.*, 2019, **109**, 666–670.

25 X. Wu, J. Xiao, R. Sun, T. Jin, J. Yang, G. Shi, Y. Wang, X. Zhang and Y. Song, Spindle-typeconjugated compounds containing twistacene unit: synthesis and ultrafast broadband reverse saturable absorption, *Adv. Opt. Mater.*, 2017, **5**(2), 1600712.

26 M. Sheik-bahae, A. A. Said, T.-H. Wei, D. J. Hagan and E. W. Van Stryland, Sensitive Measurement of Optical Nonlinearities Using a Single Beam, *IEEE J. Quantum Electron.*, 1990, **26**(4), 760–769.

27 M. Frisch, G. Trucks, H. B. Schlegel, G. Scuseria, M. Robb, J. Cheeseman, G. Scalmani, V. Barone, B. Mennucci and G. Petersson, *Gaussian 09, Revision D. 01*, Gaussian, Inc., Wallingford CT, 2009.

28 N. M. O'Boyle, A. L. Tenderholt and K. M. Langner, A Library for Package-Independent Computational Chemistry Algorithms, *J. Comput. Chem.*, 2008, **29**, 839–845.

29 T. Ahn, K. Kim, D. Kim, S. Noh, N. Aratani, C. Ikeda, A. Osuka and D. Kim, Relationship between Two-Photon Absorption and the π-Conjugation Pathway in Porphyrin Arrays through Dihedral Angle Control, *J. Am. Chem. Soc.*, 2006, **128**(5), 1700–1704.

30 Z. Xiao, Y. Shi, R. Sun, J. Ge, Z. Li, Y. Fang, X. Wu, J. Yang, M. Zhao and Y. Song, Ultrafast broadband optical limiting in simple pyrene-based molecules with high transmittance from visible to infrared regions, *J. Mater. Chem. C*, 2016, **4**, 4647–4653.

31 I. Sigmundová, P. Zahradník and D. Loos, Synthesis and study of novel benzothiazole derivatives with potential nonlinear optical properties, *Collect. Czech. Chem. Commun.*, 2007, **72**(8), 1069–1093.

32 P. Poornesh, G. Umesh, P. Hegde, M. Manjunatha, K. Manjunatha and A. Adhikari, Studies on third-order nonlinear optical properties and reverse saturable absorption in polythiophene/poly(methylmethacrylate) composites, *Appl. Phys. B*, 2009, **97**, 117–124.

33 P. Cronstrand, Y. Luo and H. Ågren, Generalized few-state models for two-photon absorption of conjugated molecules, *Chem. Phys. Lett.*, 2002, **352**, 262–269.

34 R. Sutherland, M. Brant, J. Heinrichs, J. Rogers, J. Slagle, D. McLean and P. Fleitz, Excited-state characterization and effective three-photon absorption model of two-photon-induced excited-state absorption in organic push–pull charge-transfer chromophores, *J. Opt. Soc. Am. B*, 2005, **22**(9), 1939–1948.

35 S. Delysse, P. Filloux, V. Dumarcher, C. Fiorini and J.-M. Nunzi, Multiphoton absorption in organic dye solutions, *Opt. Mater.*, 1998, **9**, 347–351.

36 S. Lee, W. Yang, J. Choi, C. Kim, S. Jeon and B. Cho, 2,6-bis[4-(p-dihexylaminostyryl)-styryl]anthracene derivatives with large two-photon cross sections, *Org. Lett.*, 2005, **7**(2), 323–326.

37 X. Wu, J. Xiao, R. Sun, J. Jia, J. Yang, G. Shi, Y. Wang, X. Zhang and Y. Song, Pyrene derivatives as broadband nonlinear optical material: magnitude and mechanism of transient refraction, *Dyes Pigm.*, 2017, **143**, 165–172.

38 Y. Shi, Z. Li, Y. Fang, J. Sun, M. Zhao and Y. Song, Ultrafast third-order nonlinear optical response of pyrene derivatives, *Opt. Laser Technol.*, 2017, **90**, 18–21.

39 Y. Zhao, H. Li, Z. Shao, W. Xu, X. Meng, Y. Song and H. Hou, Investigation of Regulating Third-Order Nonlinear Optical Property by Coordination Interaction, *Inorg. Chem.*, 2019, **58**(8), 4792–4801.

40 J. Sung, P. Kim, Y. O. Lee, J. S. Kim and D. Kim, Characterization of ultrafast intramolecular charge transfer dynamics in pyrenyl derivatives: systematic change of the number of peripheral N,N-dimethyaniline substituents, *J. Phys. Chem. Lett.*, 2011, **2**, 818–823.

41 B. Carlotti, F. Elisei, U. Mazzucato and A. Spalletti, Unusual high fluorescence of two nitro-distyrylbenzene-like compounds induced by CT processes affecting the fluorescence/intersystem-crossing competition, *Phys. Chem. Chem. Phys.*, 2015, **17**, 14740–14749.

42 H. Yılmaz, B. Küçüköz, G. Sevinç, S. Tekin, H. Yaglioglu, M. Hayvalı and A. Elmali, The effect of charge transfer on the ultrafast and two-photon absorption properties of newly synthesized boron-dipyrromethene compounds, *Dyes Pigm.*, 2013, **99**(3), 979–985.

43 R. Niu, Y. Wang, X. Wu, S. Chen, X. Zhang and Y. Song, D–π–A-Type Pyrene Derivatives with Different Push–Pull Properties: Broadband Absorption Response and Transient Dynamic Analysis, *J. Phys. Chem. C*, 2020, **124**(9), 5345–5352.

44 S. Tekin, B. Küçüköz, H. Yılmaz, G. Sevinç, M. Hayvalı, H. Yaglioglu and A. Elmali, Enhancement of two photon absorption properties by charge transfer in newly synthesized aza-boron-dipyrromethene compounds containing triphenylamine, 4-ethynyl-N,N-dimethylaniline and methoxy moieties, *J. Photochem. Photobiol., A*, 2013, **256**, 23–28.